Cylindrical nonisothermal oscillatory Couette gas flow in the slip regime: Wall shear stress and energy transfer, numerical investigation

Peter Gospodinov*, Vladimir Roussinov, Mirona Mironova

Institute of Mechanics BAS, Acad. G.Bonchev St., bl.4, 1113 Sofia, Bulgaria

Abstract

The oscillatory Couette flow between an oscillating inner cylinder and a stationary outer cylinder is considered in the study. New results for the stress and heat flux at the "gas-cylinder wall" interface are obtained. The continuum model based on the Navier-Stokes equations for compressible fluid is completed with the equations of continuity and energy transport. Along with the numerical solution proposed in our previous paper [29], it is used to investigate the cylinder-gas interaction. The wall shear stress (drag) and heat flux variation at the cylinder walls are numerically investigated. First order velocity-slip boundary conditions are specified referring to two types of motion of the inner cylinder- harmonic oscillations and stepwise oscillations. Two types of energy transfer boundary condition at inner cylinder are considered - inner cylinder with constant wall temperature and adiabatically insulated inner cylinder. Results found for the drag and heat flux variations are presented accounting for different oscillation frequencies and Knudsen numbers. Parts of the results obtained for the harmonically oscillating inner cylinder are compared to the numerical data, obtained by the DSMC method in [18]. In the case of harmonically oscillating inner cylinder a drag phase delay with respect to the wall velocity is established and studied. Hydrodynamic selfsimilarty of the drag and energy transfer variations is confirmed and analyzed.

Keywords: Rarefied gas, Compressible Navier-Stokes, Microfluidics, Numerical Methods

1. Introduction

The Couette flow in both plane and cylindrical geometry has been investigated by many authors [1], [2], [3], [4], [5], [6], [7], [8]. Recently the study of oscillatory planar Couette flow between vertically moving surfaces has become an important part of MEMS modeling [9]. Thus, Park et al. [10] presented a thorough study of oscillatory Couette flows between two parallel smooth walls, using DSMC solutions. Hadjiconstantinou [11] extended the work of [10] to include a second-order slip-flow boundary treatment. A plane oscillatory Couette flow was considered also by [13], where an analytical solution in the hydrodynamic regime was obtained. A critical analysis of theoretical and experimental data on the slip and jump coefficients available in

* Corresponding author e-mail png@imbm.bas.bg,

the open literature was presented in [21]. Tang et al [14] analyzed the effects of the Stokes and Knudsen numbers, the coefficient of tangential momentum accommodation of an oscillating Couette flow and the Stokes second problem by using lattice simulation. Based on the linearized Boltzmann equation a detailed numerical solution for a wide range of gas rarefaction and oscillatory frequency was proposed by [16]. Taheri et al [17] utilized the linearized Navier--Stokes--Fourier equations and regularized 13-moment equations to present the rarefaction effects in the plane oscillatory Couette flow. problems. Non-planar effects in an oscillatory cylindrical gas flow have been studied in [18], where an incompressible viscous flow model and the Direct Simulation Monte Carlo method were used to predict the velocity and shear stress profiles within the whole range of Knudsen number. The energy generation as a consequence of dissipation cannot be neglected even in the case of oscillating with moderate amplitude of the driven wall velocity. Recently the incompressible Navier-Stokes-Fourier (NSF) equations in the cylindrical polar coordinate reference frame were employed in [15], while the simultaneous effects of viscous dissipation and rarefaction phenomenon were taken into account. Analytical solutions for the gas and liquid velocity and temperature distribution were found in [28] for steady state one-dimensional microchannel cylindrical Couette flow between a shaft and a concentric cylinder.

In a previous paper [29] we presented numerical analysis of the continuum model of nonisothermal oscillatory cylindrical Couette gas flow in the slip regime. Our analysis was based on the continuum Navier--Stokes (NS) equations for compressible fluid completed with the equations of continuity and energy transport. Note also that nonstationary velocity, temperature and density variations were considered. Here we extend our previous investigations. Analyzing an oscillatory cylindrical Couette flow we present new results for the stress and heat flux at the gas-cylinder wall interface, and they turn to be important gas flow characteristics. We also calculate and discuss numerical

results found for the drag and heat flux variations, regarding different oscillation frequencies and Knudsen numbers that change within limits relatively wider than those specified in [29]. Along with harmonic (smooth) oscillations we consider the other limit case of stepwise (impulse) oscillations of the rotating cylinder. Yet, an arbitrary periodic movement of the rotating cylinder may find room between the two limit cases - the harmonic and the stepwise ones. Two cases of boundary conditions at the inner cylinder wall employed to solve the energy transfer equation are investigated. The first one corresponds to constant wall temperature of the inner cylinder and the second one - to an adiabatically insulated inner cylinder. The latter requirement might be important in the case of insulated cylindrical system without temperature control of the inner cylinder. A part of the results obtained for harmonic oscillations of the inner cylinder have been compared to the numerical data, obtained in the paper [18] by the DSMC method. In the case of harmonically oscillating inner cylinder a drag phase delay [10] with respect to the wall velocity is established and investigated. Noticeable heat flux variations in the gas flow are observed when the adiabatic insulated inner cylinder is investigated. The previously observed and established fact of low speeds selfsimilarity of the macroscopic flow characteristics is numerically confirmed also for drag and heat flux variations, too. The selfsimilarity with respect to the wall velocity amplitude variations allows prediction of low speed effects such as drag and heat transfer.

2. Problem formulation

The mathematical model outlined in the subsections below (2.1 an 2.2) and containing the transport equations and the correspondingly boundary conditions, is set forth in [29].

2.1. *Continuum model*

We study a rarefied hard sphere gas flow between two coaxial cylinders (one dimensional, axis-symmetric problem). The inner cylinder has radius R_1 and

peripheral velocity V_1, the outer - R_2 and V_2, respectively. The continuous model is based on the Navier–Stokes (NS) equations for compressible fluid, completed with the equations of continuity, the ideal gas low and energy transport. For details see [1], [11], [29].

The following standard notations are used: ρ for the density and T for the temperature, where **V** is the velocity vector. u and v are the velocity components along axis r and φ, P is the pressure, $\rho, P, T, u, v = f(r,t)$, $\tau_{i,j}$, $i = r, \varphi$; $j = \varphi, z$ are the stress tensor components and Φ is the dissipation function [19].

For a perfect monatomic hard sphere gas, the viscosity and heat transfer coefficients read as [20]:

(1) $\mu = \mu(T) = C_\mu \rho_0 l_0 V_0 \sqrt{T}, \quad C_\mu = \frac{5}{16}\sqrt{\pi}$.

(2) $\lambda = \lambda(T) = C_\lambda \rho_0 l_0 V_0 \sqrt{T}, \quad C_\lambda = \frac{15}{32}\sqrt{\pi}$.

The model equations are normalized by using the following scales: for density $\rho_0 = mn_0$ (m is the molecular mass, n_0 – the average number density), for velocity $V_0 = \sqrt{2RT_0}$ - R is the gas constant, for length - distance between the cylinders $L = R_2 - R_1$, for time $t_0 = L/V_0$, for temperature T_0 - the wall temperature of both cylinders. The Knudsen number is $\mathrm{Kn} = l_0/L$, where the mean free path is l_0 and $\gamma = c_P/c_V = 5/3$ (c_p and c_v are the heat capacities at constant pressure and constant volume respectively). In this way, the characteristic number Kn and the constants C_μ and C_λ take part in the dimensionless model. For brevity, hereafter the same symbols r, t, ρ, P, T, u, v and $R_i, i = 1,2$ are used for the corresponding dimensionless variables and t is the dimensionless time.

2.2 *Boundary conditions*

Following [12] and [18] the first-order slip boundary conditions, imposed at both walls, can be written directly in dimensionless form as follows

(3) $v \mp A_\sigma \mathrm{Kn}\left(\frac{\partial v}{\partial r} - \frac{v}{r}\right) = \overline{V_i}(t)$,

(4) $u = 0$,

(5) $T \pm \zeta_T \mathrm{Kn} \dfrac{\partial T}{\partial r} = 1$,

at $r = R_i,\ i = 1,2$. The upper sign in (3) and (5) corresponds $i = 1,\ r = R_1$ and the lower one to $i = 2,\ r = R_2$. For diffuse scattering we have used the viscous slip and temperature jump coefficients $A_\sigma = 1.1466$ and $\zeta_T = 2.1904$, calculated in [22] and [23] respectively using the kinetic BGK equation (see [24] for details). The same slip coefficients were used by [25], [26], [29]. Two types boundary conditions for the inner cylinder are used, when the outer one is at rest (i.e. $\bar{V}_2 = 0$).

- harmonic oscillations:

(6) $\bar{V}_1(t) = V_1 + \Delta V_1 \sin(\bar{\omega} t)$,

where $\bar{\omega}$ is the dimensionless circular frequency (the forced frequency).

- stepwise oscillations:

(7) $\bar{V}_1(t) = \begin{cases} V_1 + \Delta V_1, & 2k\pi \le \bar{\omega} t \le 2k\pi + \pi \\ V_1 - \Delta V_1, & 2k\pi + \pi \le \bar{\omega} t \le 2(k+1)\pi \end{cases}$,

where $k = 0,1,2,3....$ The dimensionless period of the oscillations t_{PER} is equal to:

(8) $t_{PER} = 2\pi / \bar{\omega}$.

In Eqs.(6), (7) V_1 is the mean wall velocity and ΔV_1 - its amplitude.

We consider in the present study circular frequencies much larger than the molecular collision frequency. The characteristic parameter θ, used in [12], to characterize the speed of oscillation $\theta = \nu_m / \omega$, connects the intermolecular collision frequency ν_m and the dimensional oscillation frequency ω. If $\theta \to 0$, the molecular collisions can be neglected.

It is convenient to introduce an additional dimensionless parameter, to describe the forced frequency influence, namely the Stokes number as given in [10], [18]:

(9) $\beta = \sqrt{\frac{\omega t_{\dim}^{\ 2}}{\nu}}$.

In Eq.(9) ω is the dimensional circular frequency, $t_{\dim}$ - the dimensional time and ν is the kinematic viscosity. Using Eq.(1), the following relation between dimensionless circular frequency $\bar{\omega}$ and Stokes number β can be written.

(10) $\bar{\omega} = C_{\mu}\mathrm{Kn}\beta^2$.

2.3. *Wall shear stress (drag) definition*

The wall shear stress or the drag is defined as dimensionless stress tensor component $\bar{\tau}_{r\varphi}$, expressing the viscous interaction between two neighboring thin "shells" of the gas medium:

(11) $\bar{\tau}_{r\varphi} = \tau_{r\varphi} / \left(\rho_0 V_0^2\right)$,

where $\tau_{r\varphi}$ is the stress tensor component along the axis φ, according to [19], written on the driven wall, in dimensional form. Accounting for the axis-symmetric case and using the definitions in the previously section 2.1, the dimensionless stress tensor component $\bar{\tau}_{r\varphi}$ can be expressed through the dimensionless quantities v, T :

(12) $\bar{\tau}_{r\varphi} = -C_{\mu}\mathrm{Kn}\sqrt{\bar{T}}\left[r\frac{\partial}{\partial r}\left(\frac{v}{r}\right)\right]$.

2.4. *Heat flux definition*

The heat transfer measure is the heat flux in the gas media on the wall, expressed as:

(13) $q_T = -\lambda\frac{\partial T}{\partial r} = -c_p\rho_0 T_0 C_{\lambda}\mathrm{Kn}\sqrt{T}\frac{\partial T}{\partial r} = -c_p\rho_0 T_0\,\bar{q}$,

where the dimensionless heat flux $\bar{q}$ is

(14) $\bar{q} = -C_{\lambda}\mathrm{Kn}\sqrt{T}\frac{\partial T}{\partial r}$,

And λ is the heat transfer coefficient defined in Eq.(3).

2.5. *Numerical solution*

The transfer equations, together with the boundary conditions (3)-(7) written for *u*, *v*, with zero initial profiles, formulate the unsteady-state initial-boundary value problem. The initial variations for density and temperature are constant i.e. $\rho(r,t=0)=1,\ T(r,t=0)=1$.

A central implicit finite difference scheme of second order of approximation is used to solve numerically the formulated problem [25], [26]. The numerical solution is described in [29].

Everywhere in the calculations, the value $\Delta V_1 = 0.3$ of the velocity amplitude is used and $V_1 = 0$. The dimensionless cylinder radii are $R_1 = 1, R_2 = 2$. The case corresponding to Kn=0.1 is chosen to be a characteristic one. This value of the Knudsen number is close to the upper limit for the slip flow regime [10], [11]. Hence, the numerical results for different Knudsen numbers (less or larger then Kn=0.1) are put together with those found for Kn=0.1.

The difference value problem is solved starting from initial profiles for all unknown quantities and proceeding until the establishment of a steady oscillating regime. It takes commonly from about one or two periods (in the case of harmonic oscillations and relative small Stokes number - $\beta \le 4$), to 16-24 periods (in the case of stepwise oscillations and relative high Stokes number - $\beta \ge 32$). Everywhere in the figures time evolution of the numerical results for $0 \le \overline{\omega} t/(2\pi) \le 1$(where $t = 0$ is a reference time), for one period is shown after the establishment of steady oscillation.

3 Numerical results: Wall shearstress

3.1 *Harmonic oscillations*

Typical cases of harmonic oscillating inner cylinder, for two different Knudsen numbers are presented on Fig.1a, 1b, where the drag results obtained

with NS model are compared against the corresponding DSMC results (calculated also for $\Delta V_1 = 0.3$).

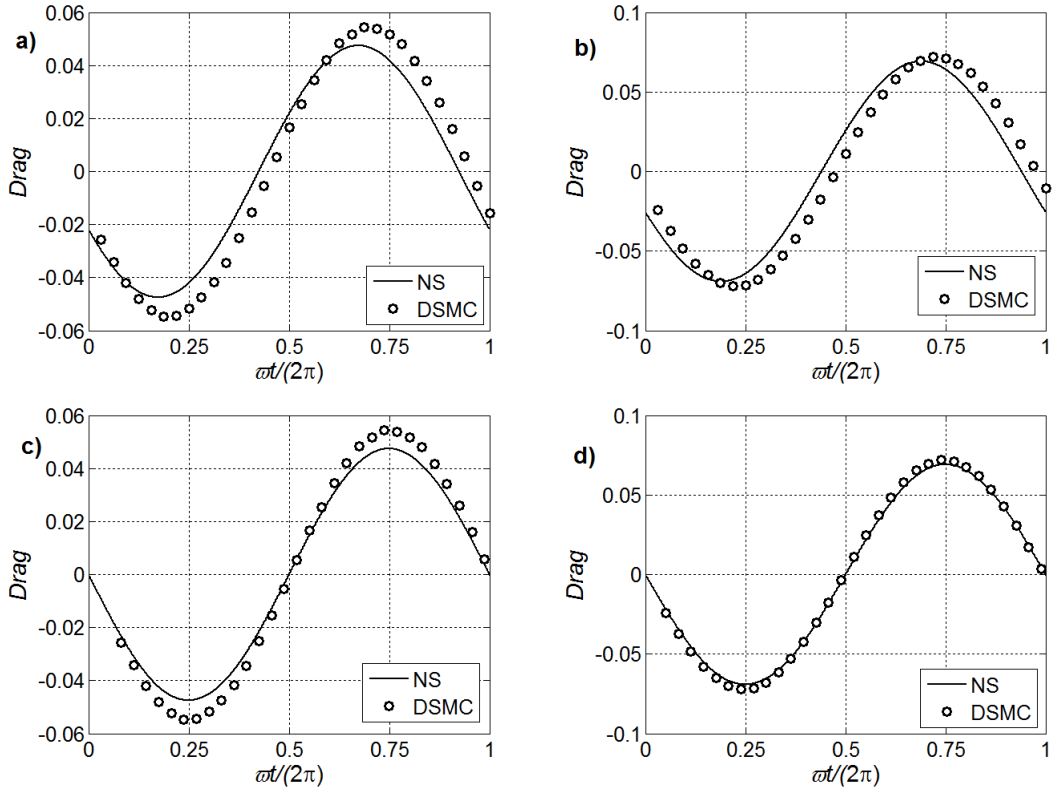

Fig.1 Harmonic oscillations – drag, comparison NS – DSMC, $\beta = 4$, $\Delta V_1 = 0.3$, $\overline{\omega} = 0.8862$ $\varphi_{1,d} = -0.075929$, $\varphi_{2,d} = -0.060179$ a) Kn=0.1 with phase delay, b) Kn=0.2 with phase delay, c) Kn=0.1 without phase delay, d) Kn=0.2 without phase delay.

The drag changes harmonically following the wall velocity change with negative sign as described in boundary condition Eq.(3). For both groups of results presented on Fig.1a, a phase delay can be observed i.e. the drag phase depends in relation to the wall velocity phase. The same results without the phase delay are plotted on fig.1b. The values of phase delay in both cases are $\varphi_{1,d} = -0.075929$ and $\varphi_{2,d} = -0.060179$.

Applying the scales introduced in section 1, the dimensionless period is defined as Eq.(8), and a new dimensionless variable τ can be introduced instead of dimensionless time *t*.

(15) $\tau = \overline{\omega} t / (2\pi)$, $0 \le \tau \le 1$, $0 \le t \le t_{per}$.

More generalized results for drag variation for different values of Knudsen number and frequencies are shown on Figs. 2a and 2b. For that purpose the mean integral drag value is introduced:

(16) $$Drag_M = \int_0^1 abs[Drag(\tau)]d\tau \ ,$$

where t_{per} is the dimensionless oscillating period and $Drag = \bar{\tau}_{r\varphi}$.

The results, presented on Fig.2 are in agreement also with the analytical solution results, presented in Emerson et al [18],

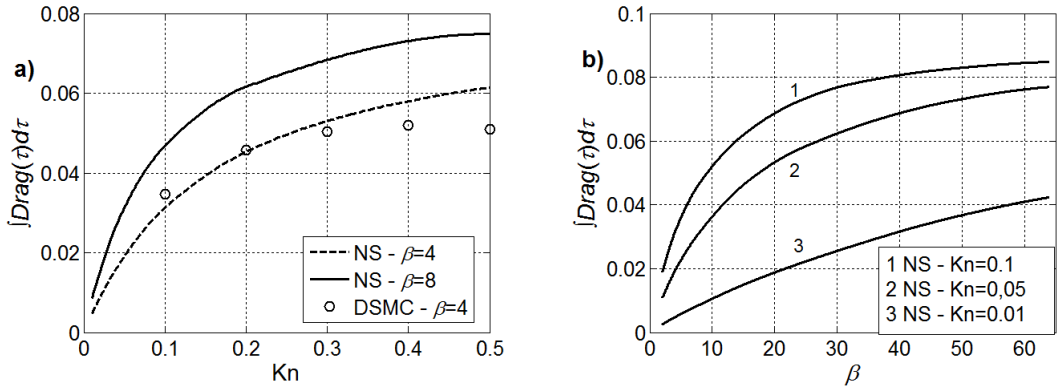

Fig.2 Drag dependencies. on Kn, a) for two fixed values of β and b) Drag dependencies on β, for three fixed Knudsen numbers

Following Park et al (2004) [10], the general representation of the velocity signal at any arbitrary coordinate *r* is expressed as:

(17) $$v(r,t) = \Delta V_1 \sin(\varpi t + \psi),$$

where ψ is the phase angle. From the slip boundary condition on the cylinder wall at $r = R_1$ follows the connection:

(18) $$\frac{A_\sigma}{C_\mu}\bar{\tau}_{r\varphi} = \Delta V_1 \sin(\varpi t) - v(R_1,t).$$

In Eq.(18) the gas velocity can be expressed using Eq.(17) or using the numerical results for $v(R_1,t)$. As seen from numerical results, plotted on Fig.3a, the gas velocity variation on the wall shows also harmonic time dependence. The $\bar{\tau}_{r\varphi}$ variation according Eq.(18) is proportional to difference between both

velocities (those of wall and gas). This difference is also presented on Fig.3a and the phase delay of the velocities difference with respect to the wall velocity is obvious. The change of the Knudsen and Stokes number cause only quantitative variation in the phase delay value. Let φ_d is the value of drag phase delay value close to the inner cylinder wall $r = R_1$

(19) $\varphi_d = \overline{\omega} t_d / (2\pi)$,

and t_d is the corresponding dimensionless delay time of drag variation toward to driven wall velocity. Note that the above described process is not observed in the case of stepwise oscillations (Fig3.b).

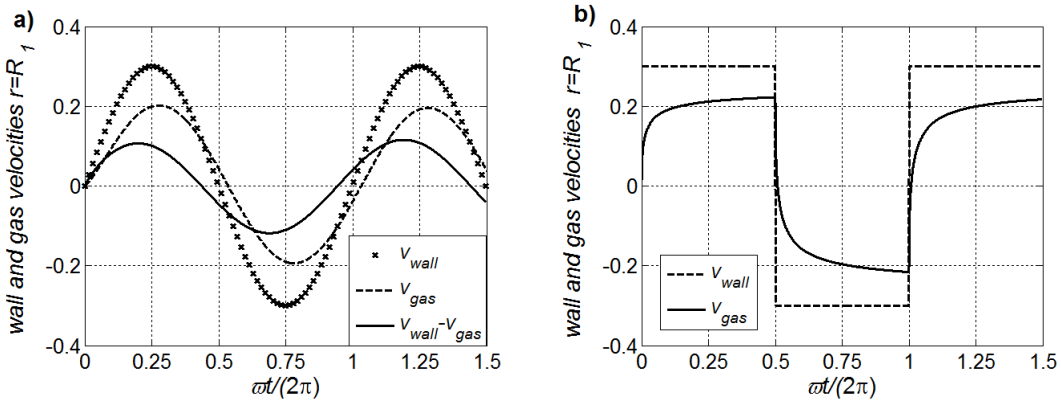

Fig.3 Velocity variation on the driven cylinder wall, $\mathrm{Kn} = 0.1$, $\beta = 4$, $\Delta V_1 = 0.3$, $\overline{\omega} = 0.8862$,
a) harmonic oscillations, b) stepwise oscillations

Fig.4a presents the relation of the drag phase delay corresponding to the case of harmonic oscillation for two fixed values of β and three fixed values of Kn. The DSMC results calculated for $\beta = 4$ and presented on the same figure confirm the phase delay existing, and are in qualitative agreement with the NS results. The phase delay dependencies for three fixed Kn numbers and $2 \le \beta \le 64$ are plotted on Fig.4b.

Hydrodynamic selfsimilarity

Our previous paper [29] established and explained the hydrodynamic similarity between velocity profiles for wall amplitude values of $\Delta V_{1,i} \le 0.3$ to

those calculated for wall amplitude values of $\Delta V_1 = 0.3$, (note that $\Delta V_{1,i}$ is the value of the velocity amplitude different from 0.3 and used in boundary condition Eq.(6) instead of ΔV_1).

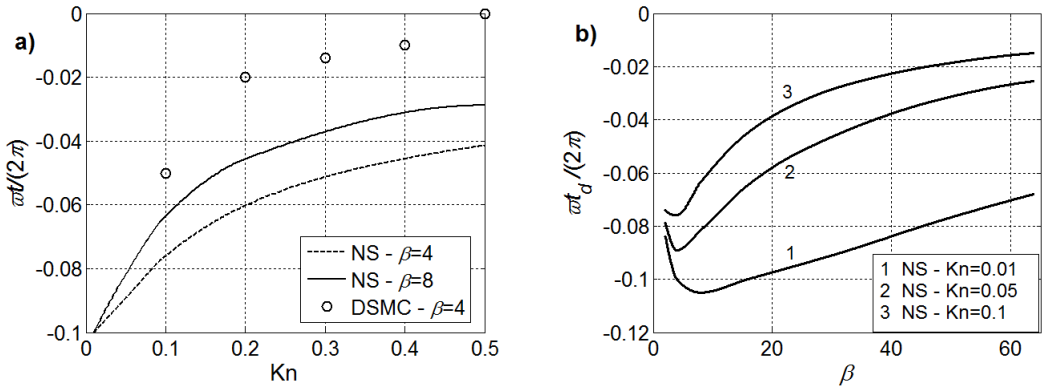

Fig.4 Harmonic oscillations – drag phase delay a) for three fixed values of β, b).for three fixed values of Kn.

The same fact is observed for the drag interaction between the gas media and the inner cylinder wall. Drag relation Eq.(12) written for $\Delta V_1 = 0.3$, can be modified for amplitude values of $\Delta V_{1,i} < 0.3$ as follows:

$$(20) \quad \bar{\tau}_{r\varphi,i} = -\frac{\Delta V_1}{\Delta V_{1,i}} C_\mu \mathrm{Kn}\sqrt{\bar{T}}\left[r\frac{\partial}{\partial r}\left(\frac{v}{r}\right)\right] = \frac{\Delta V_1}{\Delta V_{1,i}}\bar{\tau}_{r\varphi} \ .$$

For example on Fig.5 are compared the NS results, calculated for $\Delta V_{1,i} = 0.3\cdot 10^{-2}$ and scaled using Eq.(20), with NS results for $\Delta V_1 = 0.3$ and DSMC results (presented on Fig.1). The NS results after applying Eq.(20) for drag and phase delay in both cases are identical. The results confirm the hydrodynamic selfsimilarity again.

4.2. *Stepwise oscillations*

The drag variation numerical results, for two cases with different Stokes numbers (different forced oscillation frequencies) are plotted on Fig.6.. The first case $(\beta = 4)$, corresponds to this on Fig.1a, but for stepwise oscillating inner cylinder. No phase delay is established, as explained in previous subsection.

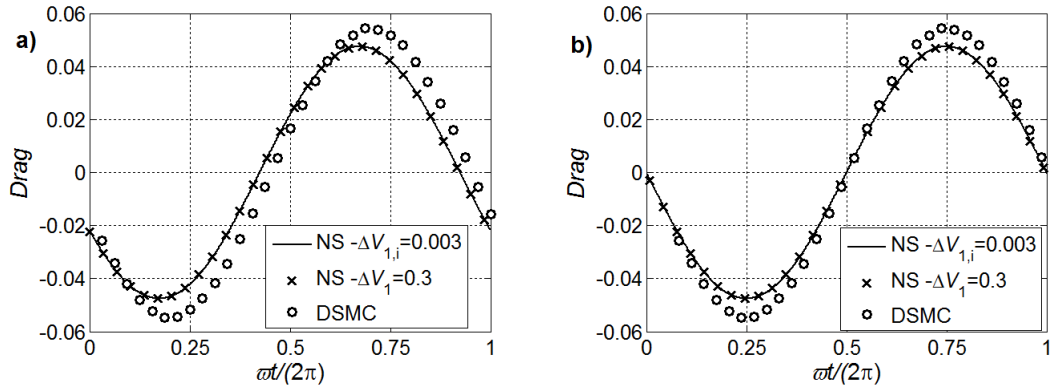

Fig.5 Selfsimilarity in drag dependencies for two different velocity amplitudes, harmonic oscillations a) with phase delay, b) without phase delay.

The numerical results for mean integral drag dependence for three fixed values of Kn and Stokes number β changing in the limits $2 \le \beta \le 128$, are presented on Fig.7.

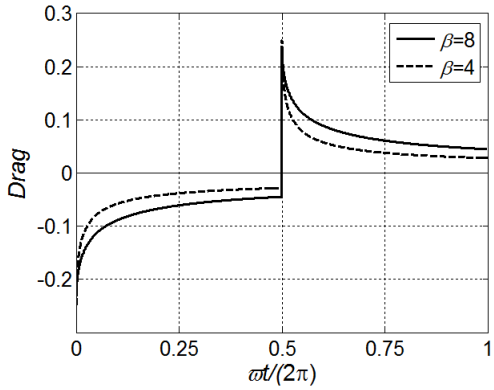

Fig.6 Stepwise oscillation: drag comparison for two forced frequencies, $\mathrm{Kn} = 0.1,\ \beta = 4,8,\ \Delta V_1 = 0.3$

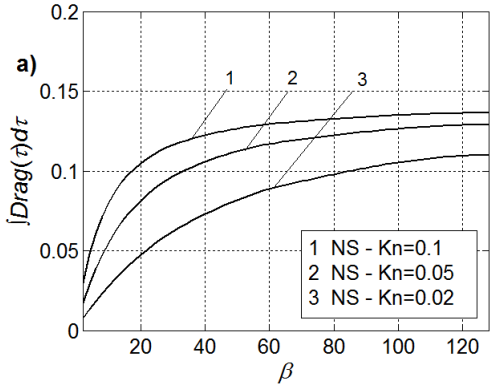

Fig.7 Mean integral drag dependencies on β, for three Knudsen values, stepwise oscillations,

Hydrodynamic selfsimilarity

The hydrodynamic selfsimilarity discussed in the previous section can be observed also in the case of stepwise oscillation. Fig.8 shows comparison between the numerical results, calculated for $\Delta V_{1,i} = 0.3 \cdot 10^{-2}$, and scaled using Eq.(20) with the results calculated for $\Delta V_1 = 0.3$. The results confirm again the existence of hydrodynamic selfsimilarity.

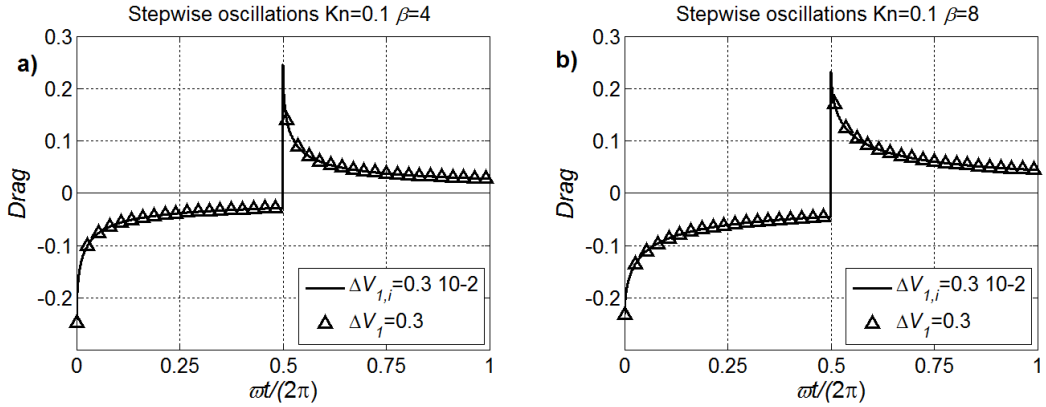

Fig.8 Selfsimilarity in drag variations, stepwise oscillations, a) $\mathrm{Kn} = 0.1,\ \beta = 4$, b). $\mathrm{Kn} = 0{,}1,\ \beta = 8$.

4. **Numerical results: Heat transfer "cylinder wall – gas media"**

In this section we analyze the energy transfer in a system "`cylinder wall--gas media'" considering both cylinders -- the oscillating inner cylinder and the static outer one. Variations of the heat flux at the inner and outer cylinder walls, regarding one period in both cases of oscillations -- harmonic and stepwise, are shown on Fig.9. The results concern the same typical cases as those, shown in Fig.1a and 6. Visible difference between the heat flux variations on the outer cylinder wall is observed when the adiabatically insulated inner cylinder is investigated -- the line marked with 3.

4.1. *Hydrodynamic selsimilarity*

The hydrodynamic selfsimilarity is valid also in the cases of heat transfer through cylinder wall. The heat flux dependence Eq.(15) written for $\Delta V_1 = 0.3$, can be modified for values of $\Delta V_{1,i} < 0.3$ as follows:

(21) $$\bar{q}_i = -\left(\frac{\Delta V_1}{\Delta V_{1,i}}\right)^2 C_k \mathrm{Kn}\sqrt{T}\frac{\partial T}{\partial r} = \left(\frac{\Delta V_1}{\Delta V_{1,i}}\right)^2 \bar{q}$$

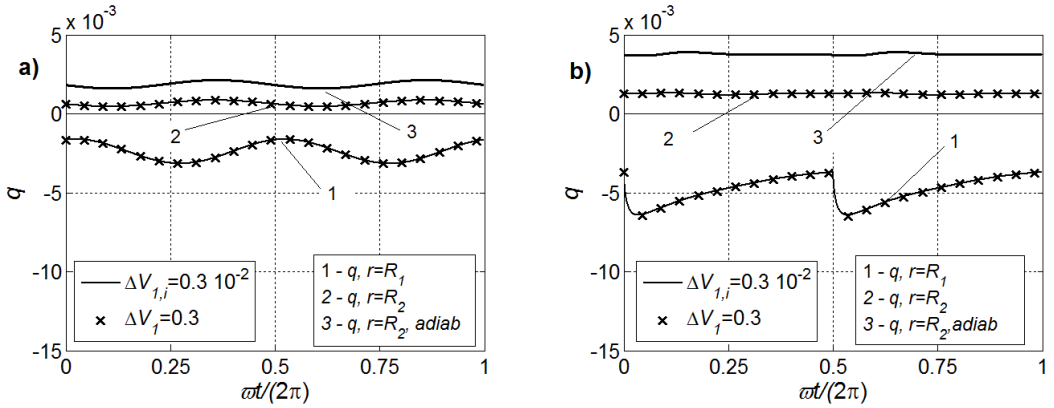

Fig.9 Heat flux, selfsmilarity, $\mathrm{Kn} = 0.1,\ \beta = 4$, a)harmonic oscillations, b) stepwise oscillations.

Note that $\bar{q}_i$ in Eq.(22) is the heatflux, calculated for velocity amplitude $\Delta V_{1,i} = 0.3 \cdot 10^{-2}$, and scaled using Eq.(21). The second power of the velocity quotient can be explained by the quadratic dependence between heat energy and fluid velocity in the dissipation function.

Based on the numerical results found for drag and heat flux for both types of inner cylinder oscillations, we may confirm and extend the conclusion of [29], stating that in the case of oscillations with relatively small velocity amplitude, neither NS nor DSMC additional computations are needed. It is sufficient to use Eq.(20) or Eq.(21) to recalculate the results once found for drag or heat flux obtained at a moderate wall velocity amplitude $\Delta V_1 = 0.3$. Regarding both types of inner cylinder wall oscillations that approach adopted with some caution, can avoid a lot of unnecessary and time consuming calculations of the viscous drag and heat energy transfer in a system "cylinder wall -- gas media" system.

As in Fig.9, Fig.10a, b shows the variation of the heat flux at the outer cylinder wall heat flux variations presented but on a larger scale. It is clearly

seen that the period of variation of dimensionless heat flux $\tau_{per} = 0.5$ is exactly twice smaller [26] then that of the driven wall velocity variation $\tau_{per} = 1$.

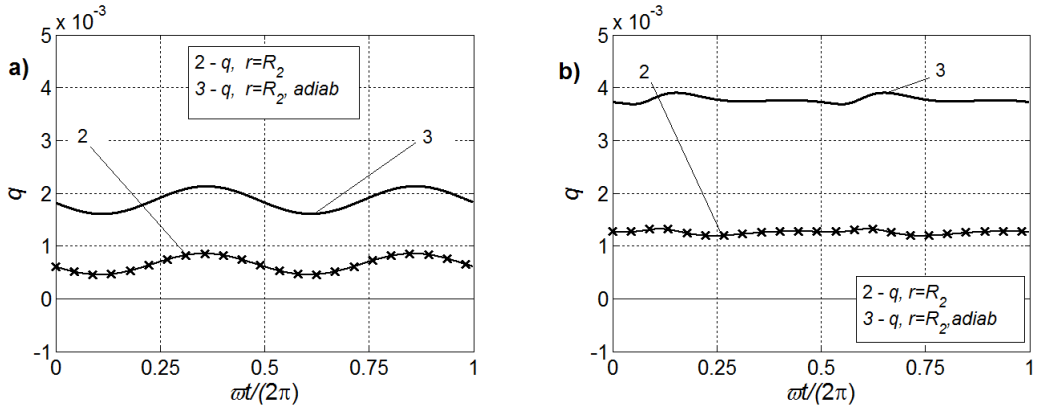

Fig.10 Outer cylinder wall heat flux:
$\mathrm{Kn} = 0.1,\ \beta = 4,\ \Delta V_1 = 0.3,\ \overline{\omega} = 0.8862,\ \omega_q = 1.7724$, a)harmonic oscillations, b) stepwise oscillations .

Using the Eq.(19) the dimensionless circular frequency of the heat flux is calculated as $\omega_q = 1.7724$. This frequency is twice larger then the forced frequency $\overline{\omega} = 0.8862$. Such a correlation can be observed for Stokes number values $\beta \le 4$ and Knudsen numbers $\mathrm{Kn} \le 0.1$ at the slip regime, for both types of oscillations of the inner cylinder. As our numerical calculations show this frequency quotient does not depend on Kn or β numbers within the above specified limits. This fact can be used to calculate the forced circular frequency in a system, where this frequency of the inner cylinder oscillations is unknown and can not be measured.

4.2. *Adiabatic insulated inner cylinder*

The case of adiabatically insulated inner cylinder [29] is a case possibly more close to the reality then the case of an inner cylinder with constant temperature. The corresponding boundary condition at the driven cylinder wall, used instead of Eq.(5) is

(22) $\dfrac{\partial T}{\partial r} = 0,\ r = R_1$.

The numerical results show difference in the temperature profiles in both cases [29], but this does not affect significantly the drag value at the oscillating cylinder wall. Hence, such results are not shown on the figures. Energy generated as a result of dissipation is transferred through the outer cylinder wall, only. The condition presented by Eq.(22) is applied, and the heat flux calculations at the outer cylinder wall are presented in Fig.9a for harmonic oscillations and in Fig.9b -for stepwise oscillations (denoted with 3). In both cases the heat energy transfer is about two times more intensive.

Heat flux mean integral value

The heat flux mean integral value is defined similarly as the drag mean value:

(23) $$q_M = \int_0^1 q(\tau) d\tau$$

The plot of the mean integral value of the heat flux vs. Stokes number in the case of a harmonically oscillating inner cylinder is shown in Fig.11a. and in the case of stepwise oscillations – on Fig.11b The heat flux moduli at both cylinder walls are of the same order of magnitude. Our qualitative comparison to DSMC results found in [29] shows, that the numerical results of the NS model solution must be examined carefully for Knudsen numbers $\mathrm{Kn} \geq 0.2$ and Stokes numbers $\beta \geq 16$.

4.3. *Gas temperature at cylinder walls: frequency and phase delay*

The numerical results provide a twice larger circular frequency of the gas temperature variations at both cylinder walls [29]. That correlation between circular frequencies does not depend on the oscillations type and the phase delay value. Gas temperature variations at the wall of a harmonic oscillating inner cylinder with and without phase delay is shown in Fig.12. A phase delay with respect to the wall velocity of the inner cylinder wall is visible analyzing gas temperature variation at the inner and outer cylinder walls.

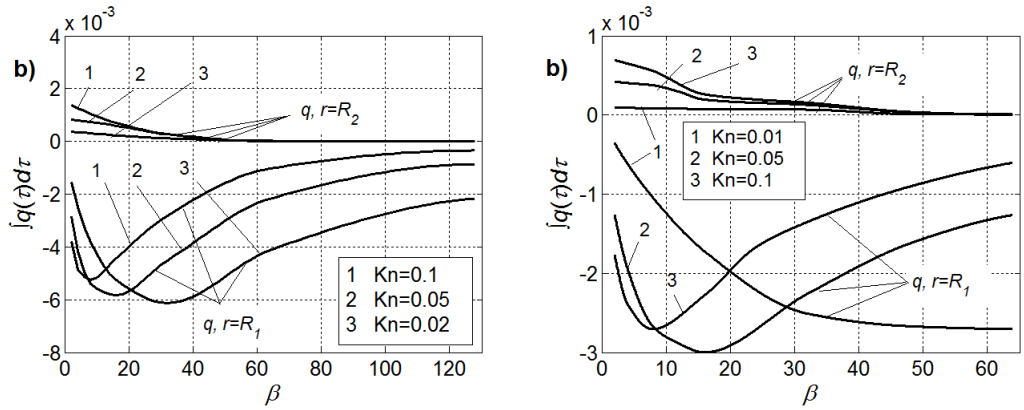

Fig,11 Mean integral heat flux dependencies, a) harmonic oscillations, b) stepwise oscillations

Analyzing the numerical results about a harmonically oscillating inner cylinder the following conclusions can be drawn: gas temperature at the inner cylinder wall has larger mean value and oscillates within relatively wider range as compared to the gas temperature at the outer cylinder wall. An opposite tendency is observed when analyzing the phase delay values. The thermal wave arising near the driven wall as a result of dissipation needs finite time to reach the outer cylinder wall. Let $\varphi_{1,d}$ be the delay of the gas velocity phase close to the inner cylinder wall and $\varphi_{2,d}$ - the delay of the gas velocity phase delay close to the outer cylinder wall, then

(24) $\varphi_{1,d} = \overline{\omega} t_{1,d} / (2\pi);\ \varphi_{2,d} = \overline{\omega} t_{2,d} / (2\pi)$,

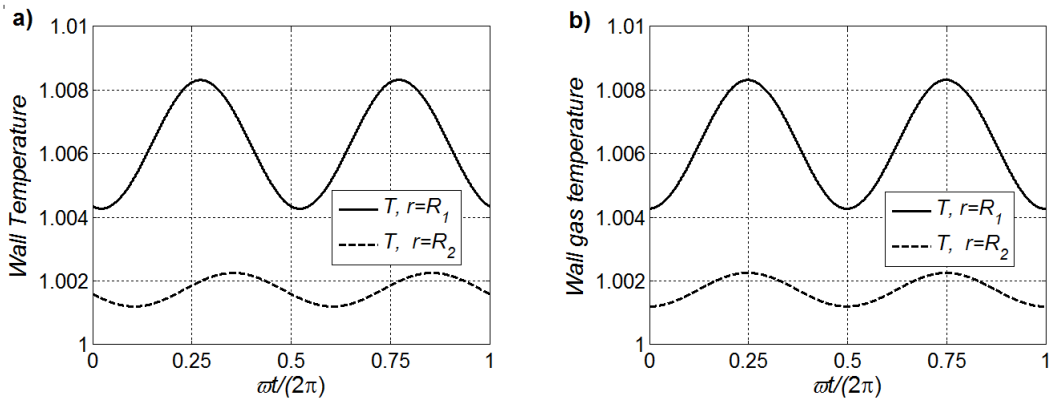

Fig.12 Gas temperature variations at the wall, $\mathrm{Kn} = 0.1,\ \beta = 4,\ \Delta V_1 = 0.3,\ \bar{\omega} = 0.8862$, harmonic oscillating inner cylinder $\varphi_{1,d} = 0.023411$, $\varphi_{2,d} = 0.10629$. a) with phase delay, b) without phase delay.

where $\varphi_{1,d}$ and $t_{2,d}$ are the corresponding dimensionless delay times. The difference

(25) $\Delta t = t_{2,d} - t_{1,d} = \frac{2\pi}{\varpi}\left(\varphi_{2,d} - \varphi_{1,d}\right)$,

is the dimensionless time needed for temperature wave to reach the outer cylinder wall.

In the case of stepwise oscillating inner cylinder no phase delay of the gas temperature variation at the inner cylinder wall is observed. At the same time, the phase delay of the gas temperature variation at the outer cylinder wall is larger then that of the case with harmonically oscillating inner cylinder.

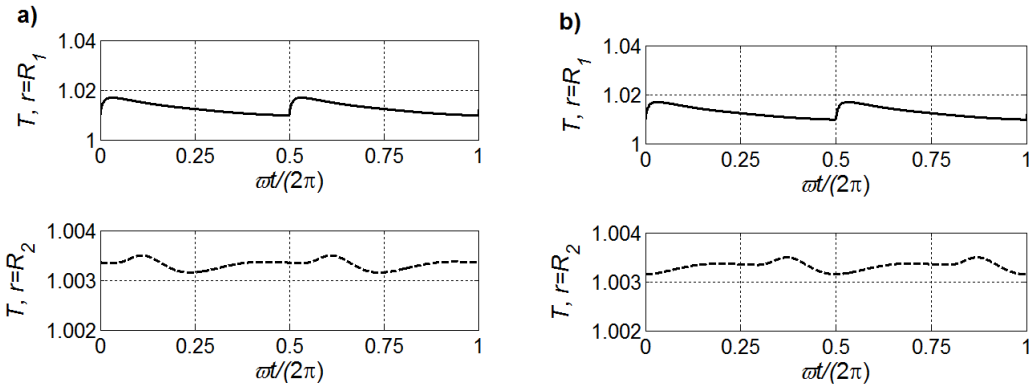

Fig.13 Wall gas temperature variations, $\mathrm{Kn} = 0.1$, $\beta = 4$, $\Delta V_1 = 0.3$, stepwise oscillating inner cylinder, $\varphi_{1,d} = 0.$, $\varphi_{2,d} = 0.23921$ a) with phase delay, b) without phase delay.

6. Conclusions

The NS model and the numerical solution found enable one to investigate numerically a cylindrical oscillatory Couette flow in two limit cases of oscillation of the active inner cylinder. The viscous interaction "`cylinder- gas"' is studied within relatively wide ranges of oscillating frequencies - Stokes number. The calculations confirm the existence of hydrodynamic selfsimilarity in drag and heat transfer in both cases of oscillation of the inner cylinder. It is also found that a phase delay of drag, wall gas temperature and heat flux variations exist in one hand and the driven wall velocity variation, in other hand. In the case of harmonically oscillating inner cylinder the drag phase delay with

respect to the driven wall velocity is numerically investigated. Visible difference in heat flux variations within the gas flow are observed when studying an adiabatically insulated inner cylinder.

Acknowledgments:

The research leading to these results has received funding from the NSF of Bulgaria under Grant No. DID 02/20-2009.

The authors would like to thank Prof. S. Stefanov for his kindness in making available some DSMC results, originally published in [18].

References

[1] C. Cercignani, F. Sernagiotto, Cylindrical Couette Flow of a Rarefied Gas, *Physics of Fluids* **10**, (1967), 1200.

[2] Y. Sone, S. Takata, T. Ohwada, Numerical analysis of the plane Couette flow of a rarefied gas on the basis of the linearized Boltzmann equation for hard-sphere molecules, *European Journal of Mechanics*, B/Fluids, **9**, (1990), 273-288.

[3] C. Cercignani, S. Cortese, Validation of a Monte Carlo simulation of the plane Couette flow of a rarefied gas, *Journal of Statistical Physics*, Volume 75, Numbers 5-6,(1994), 817-838.

[4] F. Sharipov, G. Kremer, Non-isothermal couette flow of a rarefied gas between two rotating cylinders, *European Journal of Mechanics* - B/Fluids,} **18**, (1999), 121-130.

[5] H. Yoshida, K. Aoki, Linear stability of the cylindrical Couette flow of a rarefied gas, *Phys. Rev. E*, **73**, (2006), 021201.

[6] S. Misdanitis, D. Valougeorgis, Couette flow with heat transfer in the whole range of the Knudsen number, *Proc. Of the Sixth Int. ASME Conf. of Nanochannels, Microchannels and Minichannels*, ICNMM 2008, June 23-25, Darmstadt, Germany, 2008, 1-8.

[7] E. M. Shakhov, V. A, Titarev, Numerical study of the generalized cylindrical Couette flow of rarefied gas, *European Journal of Mechanics B/Fluids*, **28**, (2009), 152--169.

[8] P. Taheri, H. Struchtrup, Effects of rarefaction in microflows between coaxial cylinders, *Phys. Rev. E*, **80**, (2009), 066317.

[9] T. Veijola, H. Kuisma, J. Lahdenpera, and T. Ryhanen, Equivalent-circuit model of the squeezed gas film in a silicon accelerometer, *Sens. Actuators A*, **48**, (1995) 239-248.

[10] J.H. Park, P. Bahukudumbi and A. Beskok, ``Rarefaction effects on shear driven oscillatory gas flows: A DSMC study in the entire Knudsen regime, *Phys. Fluids* **16**, (2004), 317.

[11] N. G. Hadjiconstantinou, Oscillatory shear-driven gas flows in the transition and free-molecular-flow regimes *Phys. Fluids*, **17**, (2005), 100611.

[12] F.Sharipov, D.Kalempa, Gas flow near a plate oscillating longitudinally with an arbitrary frequency, *Phys. Fluids*, **19**, (2007), 017110.

[13] F.Sharipov, D.Kalempa, Oscillatory Couette flow at arbitrary oscillation frequency over the whole range of the Knudsen number, *Microfluidics and Nanofluidics*, **4**, (2008), pp.363-374.

[14] G. Tang, X. Gu, R. Barber, and D. Emerson, Lattice Boltzmann simulation of nonequilibrium effects in oscillatory gas flow, *Phys. Rev***.** E, **78**, (2008), 026706.

[15] M. Shamshiri, M. Ashrafizaadeh ,E. Shirani, Investigation of flow and heat transfer characteristics of rarefied gaseous slip flow in nonplanar micro-Couette configuration, *International Journal of Thermal Sciences*, **54**, (2012), 262-275.

[16] T.Doi, Numerical analysis of oscillatory Couette flow of a rarefied gas on the basis of the linearized Boltzmann equation, *Vacuum*, **84**, (2010), 734-737.

[17] P. Taheri, A. Rana, M. Torrilhon, H. Struchtrup, Macroscopic description of steady and unsteady rarefaction effects in boundary value problems of gas dynamics, *Continuum Mech. Thermodyn*., **21**, (2009), 423–443.

[18] D. R. Emerson, Xiao-Jun Gu, S. K. Stefanov, S. Yuhong, R. W. Barber, Nonplanar oscillatory shear flow: From the continuum to the free-molecular regime, *Phys. Fluids*, **19**, (2007), 107105

[19] R. B. Bird, W. E. Stewart and E. N. Lightfoot, "Transport Phenomena", 2nd edition, John Wiley, New York, 2002.

[20] S. Chapman and T. Cowling, The mathemmatical theory of non-uniform gases, Cambride University Press, (1952).

[21] F.Sharipov, Data on the Velocity Slip and Temperature Jump on a Gas-Solid Interface *J. Phys. Chem. Ref. Data*, **40**, (2011), 023101.

[22] S. Albertoni, C. Cercignani, L. Gotusso, Numerical Evaluation of the Slip Coefficient, *Phys. Fluids*, **6**, (1963), 993 - 996.

[23] P. Bassanini, C. Cercignani, C. Pagani, Comparison of kinetic theory analyses of linearized heat transfer between parallel plates, *Int. J. Heat Mass Transfer*, **10**, (1967), 447-460.

[24] C. Cercignani, The Boltzmann equation and its applications, Springer, New York, 1988.

[25] S. Stefanov, P. Gospodinov and C. Cercignani, Monte Carlo Simulation and Navier-Stokes finite difference calculation of unsteady-state rarefied gas flows, *Physics of Fluids*, Vol.10, (1), (1998), 289-300.

[26] P. Gospodinov, D. Dankov, V. Roussinov, S. Stefanov, Modeling of cylindrical Couette flow of rarefied gas. The case of rotating outer cylinder, *First Conference of the Euro-American Consortium for Promoting the Application of Mathematics in Technical and Natural Sciences*, Sozopol, Bulgaria, *AIP Conf. Proc*., 2009, **V**, 1186, 2009.

[27] G. A. Bird, Molecular Gas Dynamics and the Direct Simulation of Gas Flows, Oxford University Press, Oxford, 1994.

[28] L.M. Jiji, A.H. Danesh-Yazdi, Flow and heat transfer in a micro-cylindrical gas-liquid Couette flow, *International Journal of Heat and Mass Transfer*, **54**, (13-14),(2011), 2913-2920.

[29] P.Gospodinov, V. Roussinov, S. Stefanov, Nonisothermal oscillatory cylindrical Couette gas flow in the slip regime:A computational study, *European Journal of Mechanics B/Fluids*, **33**, (2012), 14-24.